
<https://doi.org/10.15407/ujpe69.8.611>

L.I. MALYSHEVA

Bogolyubov Institute for Theoretical Physics,
Nat. Acad. of Sci. of Ukraine

(14b, Metrologichna Str., Kyiv 03680, Ukraine; e-mail: malysh@bitp.kiev.ua)

ON ZERO-TEMPERATURE CURRENT THROUGH AN ATOMIC CHAIN SUBJECTED TO A UNIFORMLY VARYING FIELD: GREEN'S FUNCTION FORMALISM

On the basis of the tight-binding formalism and Green's function technique, we obtain all matrix elements of Green's functions for a biased chain with linear variations of the electron on-site energy. Their dependence on system parameters is analyzed in the context of through-molecule electron transport.

Keywords: electron transport, Green's functions, transmission coefficient.

1. Introduction

During the last decades, the process of fabrication of various molecular contacts of the “metal–molecular system–metal” type has received the impressive experimental development allowing high-precision measurements of electric current through single molecules, nanotubes, self-assembled monolayers, and nanometer-size dielectric and semiconductor films. However, the interpretation of these experiments based on the Landauer concept of conductance requires, as a rule, the use of computational simulations of molecular electronic structures. These studies often give quite limited and method-dependent information, which stimulates the development of analytic approaches to the investigation of the electric properties of molecular contacts.

Citation: Malysheva L.I. On zero-temperature current through atomic chain subjected to a uniformly varying field: Green's function formalism. *Ukr. J. Phys.* **69**, No. 8, 611 (2024). <https://doi.org/10.15407/ujpe69.8.611>.

© Publisher PH “Akademperiodyka” of the NAS of Ukraine, 2024. This is an open access article under the CC BY-NC-ND license (<https://creativecommons.org/licenses/by-nc-nd/4.0/>)

In the present paper, we use the analytic derivation of the transmission coefficient $T(E, V)$, the ratio of the transmitted electron flux to incident flux for a given energy E and applied voltage V , in terms of the coupling function matrix [1–10]. This matrix is determined by the Green functions of ideal leads and molecule-lead interaction matrix. We will apply the formulation used in [7], which exactly describes molecular contacts with the use of realistic model Hamiltonians. Thus, we use the exact analytic expression for the transmission coefficient obtained for a three-dimensional lead modeled by a cubic semiinfinite lattice with an arbitrary number of atoms on the surface and in subsurface layers interacting with the molecule [3].

In the 1960s, Wannier introduced the concept of electron energy quantization in solids subjected to the action of constant homogeneous electric fields [11, 12]. Actually, his concept was formulated for an infinite monatomic chain described in the Wannier tight-binding approximation. It can be considered as the theory of Stark effect for a chain of interacting single-level atoms. Therefore, the obtained electron spectrum was called a Wannier–Stark ladder or

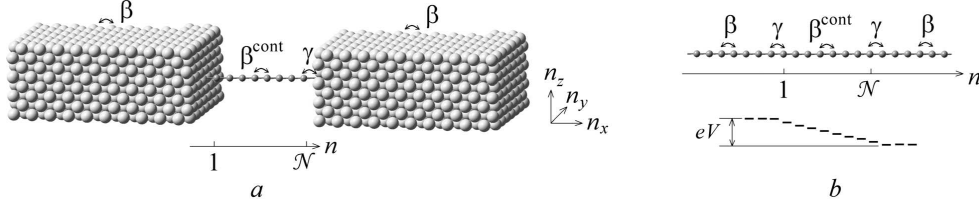


Fig. 1. Fragments of semiinfinite (in the n_x direction) left and right leads with a molecular chain in between. The binding atoms of the chain are in the on-top position. The energies of electron transfer between adjacent atoms are β in the leads, β^{cont} in the molecular chain, and γ on the electrode-molecule interface (a). One-dimensional case, $N_y = N_z = 1$ (b)

the WS quantization of the electron energy, namely, $E_\mu = \mu\varepsilon$, where μ is an integer. The field parameter ε ($-\varepsilon$) determines the variations of the electron potential energy from an atom to the next atom along (against) the field.

Numerous accurate explicit expressions showing the electric-field effects on the chain electron spectrum were derived in [7, 13–21]. The polynomial representation of the exact solution to the spectral problem for the field-affected \mathcal{N} -atom long tight-binding chain [22] was obtained in the context of through-molecule transport.

In what follows, we present all explicit expressions for the matrix elements of the Green functions for a biased chain with linear variations of the electron on-site energy derived from the exact characteristic equation for the Hamiltonian matrix of the \mathcal{N} -length atomic chain. The obtained results are used to deduce an explicit expression for the transmission coefficient of electrons through a spatially finite tilted band. It reveals the resonance structure of the transmission spectrum and its dependence on the characteristic parameters of the system.

2. Transmission Coefficient

We consider a metal wire connected to a scattering region, but, otherwise, ideal in a sense that, in the absence of imperfections, electrons can flow freely along the wire. Assume that, as shown in Fig. 1, a, there is a molecule coupled in a certain way with the left and right parts of the wire (the left and right leads) playing the role of imperfection. Within the framework of the Landauer–Büttiker theory [23–25], the transmission probability is directly related to the current-voltage relation. For the efficient computation and analytic description of the transmission coefficient, the Green function technique proves to be es-

pecially useful for the development of reliable computational schemes. In [26], it was proposed to describe the tunnel current in metal–insulator–metal heterostructures by using the Green-function language. Later, their treatment was reformulated in numerous physical contexts to examine, in particular, the quantum conductance of molecular wires [3, 13–17].

Within the framework of the Green-function formalism, $T(E, V)$ can be expressed in terms of the Green functions related to the noninteracting left and right leads and the scattering region. To find $T(E, V)$, we make our model more specific as follows: In the bra-ket notation, $|\mathbf{n}\rangle \equiv a_{\mathbf{n}}^+|0\rangle = a_{n_x}^+ a_{n_y}^+ a_{n_z}^+|0\rangle$, $\langle \mathbf{n}|\mathbf{n}'\rangle = \delta_{\mathbf{n},\mathbf{n}'}$, the Hamiltonian of the system “left lead-molecular contact-right lead” depicted in Fig. 1 takes the form

$$\hat{H} = \hat{H}^L + \hat{H}^{\text{cont}} + \hat{H}^R + \hat{H}^{\text{int}}. \quad (1)$$

Figure 1 explains the model parameters and shows the potential profile on the electron way from the left electrode to the right one. We assume that, in the absence of interaction between the left/right leads and the contact, the eigenstates Ψ^μ of the Hamiltonian operators \hat{H}^μ of the leads and the contact ($\mu = L, R$, and contact, respectively) can be expanded in a series in the respective basis set of atomic orbitals $\Psi^\mu = \sum_{\mathbf{n} \in \mathbf{n}_\mu} \psi_{\mathbf{n}}^\mu |\mathbf{n}\rangle$. We also treat the Hamiltonians \hat{H}^L and \hat{H}^R used to describe the leads, as free electron Hamiltonians of semiinfinite cubic lattices with the hopping integral between the nearest-neighbor atoms denoted by $-\beta$ ($\beta > 0$). Thus, the energy of transmitted waves is

$$E(k_{j_y, j_z}) = 6\beta - 2\beta[\cos(k_{j_y, j_z}) + \cos(\xi_y) + \cos(\xi_z)], \quad (2)$$

$$\xi_{(y,z)} \equiv \frac{\pi j_{(y,z)}}{N_{(y,z)} + 1}, \quad j_{(y,z)} = 1, \dots, N_{(y,z)},$$

where k_{j_y, j_z} is real (imaginary) for propagating (evanescent) modes.

The left-to-right drop of the applied potential eV is taken into account as a shift of the site energies of each atom by the field parameter $\varepsilon = eFa/\beta$, where e is the absolute value of the electron charge, F is the electric-field strength, and a is the lattice constant. Thus, we have assumed that the potential difference between the left and right electrodes linearly decreases inside the contact: $eV = \varepsilon(\mathcal{N} + 1)$, and the Hamiltonian of molecular chain takes the form

$$\hat{H}^{\text{cont}} = \sum_{n=1}^{\mathcal{N}} \left\{ (\varepsilon^{\text{cont}} - n\varepsilon) a_n^+ a_n - \beta^{\text{cont}} [(1 - \delta_{n,1}) a_{n-1}^+ + (1 - \delta_{n,\mathcal{N}}) a_{n+1}^+] a_n \right\}. \quad (3)$$

We consider a simplified model of metal-molecular interaction, which involves only two atoms in the entire collection of molecule atoms: these binding atoms have the coordinates $n = 1$ and $n = \mathcal{N}$. The interaction operator is then given by

$$\hat{H}^{\text{int}} = \gamma \sum_{\mathbf{n} \in \mathbf{n}_L} |1\rangle \langle \mathbf{n}| + \gamma \sum_{\mathbf{n} \in \mathbf{n}_R} |\mathcal{N}\rangle \langle \mathbf{n}|, \quad (4)$$

i.e., the parameter γ determines the difference between the electron transfer rates from the contact to the electrodes and backward.

By definition, the transmission coefficient is equal to the ratio of the transmitted electron flux to the incident flux. The procedure of derivation of the transmission coefficient is well known [1–3, 7]. Due to the simplifying model assumptions, this principal quantity can be obtained in the fully analytic form by solving the Lippman–Schwinger equation with the Hamiltonian \hat{H} . Here, we use $T(E, eV)$ in the following form:

$$T(E, eV) = 4\text{Im}(A^L)\text{Im}(A^R)(G_{1,\mathcal{N}}^{\text{cont}})^2 \left| (1 - A^L G_{1,1}^{\text{cont}}) \times \right. \\ \left. \times (1 - A^R G_{\mathcal{N},\mathcal{N}}^{\text{cont}}) - A^L A^R (G_{1,\mathcal{N}}^{\text{cont}})^2 \right|^{-2}, \quad (5)$$

where $G_{n,n'}^{\text{cont}}$ are the Green functions for Hamiltonian (3), the coupling functions A^L and A^R are given by the formulas

$$A^{(L,R)} = \gamma^2 \sum_{\mathbf{n}, \mathbf{n}' \in \mathbf{n}_{(L,R)}} G_{\mathbf{n}, \mathbf{n}'}^{(L,R)},$$

and the Green functions of the left and right leads for $n_x = n_{x'} = 1$ are as follows:

$$G_{1,n_y, n_z; 1, n'_y, n'_z}^{(L,R)} = -\frac{1}{\beta} \frac{4}{(N_y + 1)(N_z + 1)} \times \\ \times \sum_{j_y=1}^{N_y} \sum_{j_z=1}^{N_z} e^{ik_{j_y, j_z}^{(L,R)}} \sin(\xi_y n_y) \sin(\xi_z n_z) \times \\ \times \sin(\xi_y n'_y) \sin(\xi_z n'_z). \quad (6)$$

To find the transmission coefficient for the model specified by the Hamiltonian operator in Eq. (3), it is necessary to know the matrix elements of the Green functions appearing in Eq. (5). They are found in the next section. In what follows, the model parameters $\varepsilon^{\text{cont}}$, β^{cont} , γ , and ε are expressed by using β as the unit of energy.

3. Green's Functions for a Tilted Chain in the Tight-Binding Model

The system of equations for finding the required Green functions has the form

$$(E - \varepsilon^{\text{cont}} + n\varepsilon) G_{n,n'}^{\text{cont}} = -\beta^{\text{cont}} [(1 - \delta_{n,1}) G_{n-1,n'}^{\text{cont}} + \\ + (1 - \delta_{n,\mathcal{N}}) G_{n+1,n'}^{\text{cont}}] + \delta_{n,n'}, \quad (7)$$

where $n, n' = 1, \dots, \mathcal{N}$. To find all matrix elements $G_{n,n'}^{\text{cont}}$, it is convenient to use the method of generating functions. We define the generating function as follows:

$$\mathcal{G}_{n'}(\varphi) = \sum_{n=1}^{\mathcal{N}} G_{n,n'}^{\text{cont}}(E, eV) e^{in\varphi}. \quad (8)$$

It can be shown by direct substitution that $\mathcal{G}_{n'}(\varphi)$ satisfies the following differential equation:

$$(E - \varepsilon^{\text{cont}} + 2\beta^{\text{cont}} \cos \varphi) \mathcal{G}_{n'}(\varphi) - i\varepsilon \frac{d\mathcal{G}_{n'}(\varphi)}{d\varphi} = \\ = e^{in'\varphi} + \beta^{\text{cont}} G_{1,n'}^{\text{cont}} + \beta^{\text{cont}} e^{i(\mathcal{N}+1)\varphi} G_{\mathcal{N},n'}^{\text{cont}}. \quad (9)$$

Solving this linear differential equation allows us to express the solution of (7) in terms of the Bessel functions of the first and second kinds $J_\nu(z)$ and $Y_\nu(z)$. Namely, the solution has the form

$$G_{n,n'}^{\text{cont}}(E, eV) = \\ = -\frac{\pi}{\varepsilon [J_\nu(z) Y_{\nu-\mathcal{N}-1}(z) - J_{\nu-\mathcal{N}-1}(z) Y_\nu(z)]} \times$$

$$\times \begin{cases} [J_{\nu-n}(z)Y_{\nu-N-1}(z) - J_{\nu-N-1}(z)Y_{\nu-n}(z)] \times \\ \times [J_{\nu}(z)Y_{\nu-n'}(z) - J_{\nu-n'}(z)Y_{\nu}(z)], & n \geq n', \\ n \leftrightarrow n', & n \leq n', & z = \frac{2\beta^{\text{cont}}}{\varepsilon}, \\ \nu = -(E - \varepsilon^{\text{cont}})\frac{\mathcal{N}+1}{eV} = -(E - \varepsilon^{\text{cont}})\frac{1}{\varepsilon}. \end{cases} \quad (10)$$

For the particular values of n , $n' = 1$, \mathcal{N} , Eq. (10) gives the expressions for the Green functions used in the definition of the transmission coefficient $T(E, eV)$:

$$\begin{aligned} \mathcal{D}_G(E, eV)G_{1,1}^{\text{cont}}(E, eV) &= \\ &= J_{\nu-1}(z)Y_{\nu-N-1}(z) - Y_{\nu-1}(z)J_{\nu-N-1}(z) \equiv \tilde{G}_{1,1}, \\ \mathcal{D}_G(E, eV)G_{\mathcal{N},\mathcal{N}}^{\text{cont}}(E, eV) &= \\ &= J_{\nu}(z)Y_{\nu-N}(z) - Y_{\nu}(z)J_{\nu-N}(z) \equiv \tilde{G}_{\mathcal{N},\mathcal{N}}, \\ \mathcal{D}_G(E, eV)G_{1,\mathcal{N}}^{\text{cont}}(E, eV) &= \frac{1}{\pi} \frac{\varepsilon}{\beta^{\text{cont}}} \equiv \tilde{G}_{1,\mathcal{N}}, \quad (11) \\ Q(E, eV) &= \mathcal{D}_G(E, eV) \left\{ G_{1,1}^{\text{cont}}(E, eV)G_{\mathcal{N},\mathcal{N}}^{\text{cont}}(E, eV) - \right. \\ &\quad \left. - [G_{1,\mathcal{N}}^{\text{cont}}(E, eV)]^2 \right\} = \\ &= \frac{-1}{\beta^{\text{cont}}} [J_{\nu-1}(z)Y_{\nu-N}(z) - Y_{\nu-1}(z)J_{\nu-N}(z)], \end{aligned}$$

and

$$\mathcal{D}_G(E, eV) = -\beta^{\text{cont}} [J_{\nu}(z)Y_{\nu-N-1}(z) - Y_{\nu}(z)J_{\nu-N-1}(z)]. \quad (12)$$

Note that, for $\mathcal{N} = 1$, by using the well-known relations for the Bessel functions

$$\begin{aligned} J_{\nu-1}(z)Y_{\nu-2}(z) - Y_{\nu-1}(z)J_{\nu-2}(z) &= \frac{2}{\pi z}, \\ \left\{ \begin{matrix} J \\ Y \end{matrix} \right\}_{\nu-1}(z) + \left\{ \begin{matrix} J \\ Y \end{matrix} \right\}_{\nu+1}(z) &= \frac{2\nu}{z} \left\{ \begin{matrix} J \\ Y \end{matrix} \right\}_{\nu}(z), \end{aligned}$$

in Eqs. (11) and (12), we obtain the following evident relation:

$$G_{1,1}^{\text{cont}}(E, eV) = \frac{1}{E - (\varepsilon^{\text{cont}} - eV/2)}. \quad (13)$$

Relations (10) give analytic expressions for the Green functions for a biased linear chain which can be used for analytic modeling in a great number of applications. Substituting Eqs. (11) in Eq. (5), we can find the transmission coefficient for the system presented in Fig. 1. In the next section, we will use these results to derive $T(E, eV)$ for the case $N_y = N_z = 1$, i.e., for an atomic chain depicted in Fig. 1, *b*.

614

4. One-Dimensional Case

4.1. Transmission coefficient

For the case $N_y = N_z = 1$, our model corresponds to the atomic chain shown in Fig. 1, *b*. The site energy along the chain is equal to 2 (to recall, in β units) for $n_x \leq 0$, to $2 - eV$ for $n_x > \mathcal{N}$, and to $2 - \varepsilon n$, $\varepsilon = eV/(\mathcal{N} + 1)$ for $n \in \overline{1, \mathcal{N}}$ in the left and right electrodes and in the contact, respectively. The eigenenergies (2) for Hamiltonian (1) are simplified in this case to

$$E = 2(1 - \cos k^L) = 2(1 - \cos k^R) - eV, \quad (14)$$

$0 \leq k^L, k^R \leq \pi$, with the wave vectors in units of the inverse interatomic distance a^{-1} . Relation (5) can be now rewritten as follows:

$$\begin{aligned} T(E, eV) &= 4\gamma^4 \sin k^L \sin k^R (G_{1,\mathcal{N}}^{\text{cont}})^2 \times \\ &\times \left| 1 + \gamma^2 \left(e^{ik^L} G_{1,1}^{\text{cont}} + e^{ik^R} G_{\mathcal{N},\mathcal{N}}^{\text{cont}} \right) + \right. \\ &\quad \left. + \gamma^4 e^{i(k^L+k^R)} \left[G_{1,1}^{\text{cont}} G_{\mathcal{N},\mathcal{N}}^{\text{cont}} - \left(G_{1,\mathcal{N}}^{\text{cont}} \right)^2 \right] \right|^{-2}. \quad (15) \end{aligned}$$

By using relations for the Green functions (11), after some algebra, we get

$$\begin{aligned} \mathcal{D}_T T(E, eV) &= 4\gamma^4 \sin k^L \sin k^R \tilde{G}_{1,\mathcal{N}}^2, \\ \mathcal{D}_T &\equiv \left[\mathcal{D}_G + \gamma^2 \left(\cos k^L \tilde{G}_{1,1} + \cos k^R \tilde{G}_{\mathcal{N},\mathcal{N}} \right) + \right. \\ &\quad \left. + \gamma^4 \cos(k^L - k^R) Q(E, eV) \right]^2 + \\ &\quad + \gamma^4 \left[\sin k^L \tilde{G}_{1,1} - \sin k^R \tilde{G}_{\mathcal{N},\mathcal{N}} + \right. \\ &\quad \left. + \gamma^2 \sin(k^L - k^R) Q(E, eV) \right]^2 + \\ &\quad \left. + 4\gamma^4 \sin k^L \sin k^R \tilde{G}_{1,\mathcal{N}}^2. \end{aligned} \quad (16)$$

The condition of transmission without backscattering, $T(E, eV) = 1$, directly follows from Eq. (16):

$$\begin{aligned} &\left[\gamma^{-2} \mathcal{D}_G + \cos k^L \tilde{G}_{1,1} + \cos k^R \tilde{G}_{\mathcal{N},\mathcal{N}} + \right. \\ &\quad \left. + \gamma^2 \cos(k^L - k^R) Q(E, eV) \right]^2 + \\ &\quad + \left[\sin k^L \tilde{G}_{1,1} - \sin k^R \tilde{G}_{\mathcal{N},\mathcal{N}} + \right. \\ &\quad \left. + \gamma^2 \sin(k^L - k^R) Q(E, eV) \right]^2 = 0. \quad (17) \end{aligned}$$

In the particular case, $\beta^{\text{cont}} = 1$ and $eV = 0$ (and, hence, $k^L = k^R = k$), Eq. (16) repeats the result obtained in [7]:

$$T(E, 0) = 4\gamma^4 \sin^4 k \left\{ \left[\sin(\mathcal{N} + 1)k - 2\gamma^2 \cos k \sin \mathcal{N}k + \gamma^4 \sin[(\mathcal{N} - 1)k] \right]^2 + 4\gamma^4 \sin^4 k \right\}^{-1}. \quad (18)$$

For the single-atom contact $\mathcal{N} = 1$, we easily get $\varepsilon = eV/2$, $G_{1,1} = 1$, and $\mathcal{D}_G = E - 2 + eV/2$. Then Eq. (16) can be represented in the explicit form

$$\begin{aligned} T(E, eV) &= 2\gamma^4 R \left\{ 2(E - 2 + eV/2)^2 (1 - 2\gamma^2) + \right. \\ &\quad \left. + \gamma^4 [4 + (2 - E)(2 - E - eV) + R] \right\}^{-1}, \\ R &\equiv \sqrt{E(4 - E)} \sqrt{(E + eV)(4 - E - eV)}, \\ T(E, 0) &= \frac{\gamma^4 E(4 - E)}{(E - 2)^2 (1 - 2\gamma^2) + 4\gamma^4}. \end{aligned} \quad (19)$$

For $\mathcal{N} \geq 2$, the analogues of Eqs. (19) are too cumbersome to be presented.

Expression (16) is much simpler than Eq. (5), but still remains quite complicated. However, in the case of small potential difference, $eV \ll 1$, it can be significantly simplified with the help of an approximation similar to that used in [20]. Namely, for any coupling parameter γ and any \mathcal{N} , the transmission coefficient $T(E, eV)$ can be approximated as follows:

$$T(E, eV) \approx 4\gamma^4 \left\{ 4\gamma^4 + (1 - \gamma^4)^2 \times \sin^2 \left[p + \frac{\mathcal{N} + 1}{2} \left(E - 2 + \frac{eV}{2} \right) \right] \right\}^{-1}, \quad (20)$$

where

$$p \equiv \frac{\pi}{4} [(-1)^\mathcal{N} + 1].$$

In the next subsection, we apply the obtained results to find the volt-ampere characteristics of the considered “left lead-contact-right lead” system.

4.2. Volt-ampere characteristics

Following the Landauer–Büttiker theory [23, 24], we express the current-voltage relation via the transmission coefficient in the form

$$I(eV) = \frac{2e}{h} \int_{\max(0, 2 - eV)}^{\min(2, 4 - eV)} T(E, eV) dE. \quad (21)$$

The limits of integration $[2 - eV, 2]$, $0 \leq eV \leq 2$ and $[0, 4 - eV]$, $2 \leq eV \leq 4$ correspond to the nonzero values of the transmission coefficient specified by the Pauli exclusion principle.

The volt-ampere characteristics presented in Figs. 2–4 are computed by using the exact expression for the transmission coefficient (16). In all presented plots, the energies are expressed in the units of β (the absolute value of the hopping integral between the nearest-neighbor atoms of the leads). Within the framework of the nearest-neighbor tight-binding model, the bandwidth is 12β and 4β in three dimension and one dimension, respectively. Then if the metallic bandwidth is assumed to be of an order of 10 eV, we can use $\beta \sim 1$ eV for the three-dimensional model of the leads depicted in Fig. 1, *a* and $\beta \sim 2.5$ eV in the one-dimensional case (Fig. 1, *b*).

The choice of the dimensionless parameters γ (metal-contact interaction) and β^{cont} (interaction in the tilted chain) depends on the specific molecular system. For our calculations, we chose the following two sets of parameters: $\beta^{\text{cont}} = 1$ with several values of γ (Figs. 2 and 4), and $\beta^{\text{cont}} = \gamma$ (Fig. 3). Thus, the first set can be used, in particular, to describe the electron transport in the one-dimensional case, if the hopping integral between the atoms of molecular chain is of an order of 2.5 eV, which is typical, e.g., of the graphene-based chain. The second set can be applicable to the estimation of the conduction properties of single molecule junction (see, e.g., [8]) or terminated alkane chains (see, e.g., [10]).

The top panel row in Fig. 2 shows the I–V characteristics for contacts with the numbers of atoms $\mathcal{N} = 1, 9, 49$, which are perfectly ($\gamma = 1$) and weakly ($\gamma = 0.5, 0.25$) coupled with the emitter and the collector. The bottom panel row represents $I(eV)$ for $\mathcal{N} = 3, 5, 7$ and $\gamma = 1, 0.25, 0.1$.

The volt-ampere characteristic plotted in Fig. 2, which corresponds to $\mathcal{N} = 49$, and $\gamma = 1$, has the shape of an isosceles triangle. For $\mathcal{N} \lesssim 10$, the perfect triangular I–V shape is deteriorated only slightly and basically remains unchanged. The difference between the I–V characteristics of contacts with lengths $9 \lesssim \mathcal{N} \lesssim 49$ becomes negligible, while, for $\mathcal{N} \gtrsim 49$, the dependence of I on eV does not change for all accessible levels of the accuracy of numerical integration. This conclusion is equally valid for the odd and even numbers of atoms in the contact.

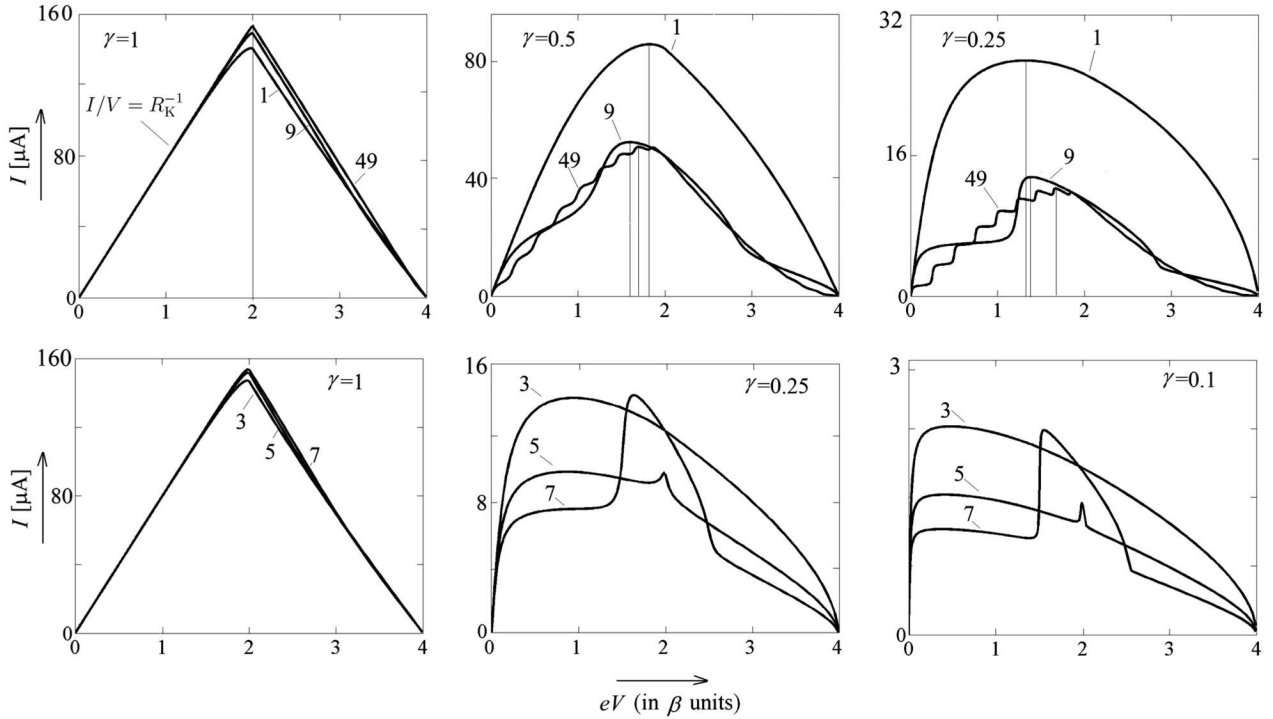


Fig. 2. I–V characteristics of contacts of lengths $\mathcal{N} = 1, 9, 49$ (top panel row) and $\mathcal{N} = 3, 5, 7$ (bottom panel row) for different values of γ and $\beta^{\text{cont}} = 1$. The left side of perfect isosceles triangle ($\mathcal{N} = 49, \gamma = 1$) corresponds to the volt-ampere characteristic $I = \frac{2e^2}{h}V, h/(2e^2) = 12.9k\Omega$

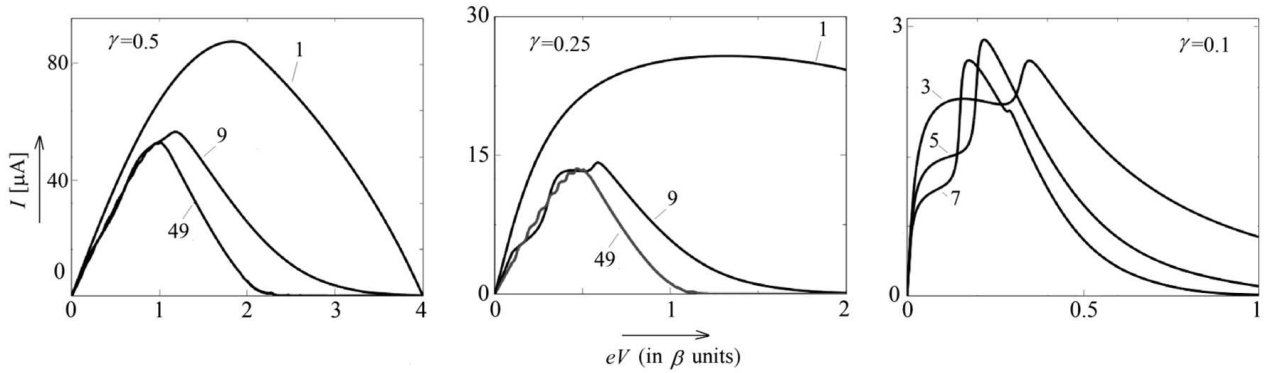


Fig. 3. I–V characteristics of contacts of lengths $\mathcal{N} = 1, 9, 49$ (left and middle panels) and $\mathcal{N} = 3, 5, 7$ (right panel) for different values of γ and $\beta^{\text{cont}} = \gamma$. The curve for $N = 49$ in the middle panel is marked with red color for clarity

Weak coupling exemplified in Fig. 2 for $\gamma = 0.5, 0.25$, and 0.1 , qualitatively changes the volt-ampere characteristics of perfectly coupled atomic wire. First, for contacts with any number of atoms, the shape of I–V curves has nothing common with the triangle. Second, for each particular value of $N < 10$, the dependence $I(eV)$ is unique. The only common feature is

that the ohmic current can be observed for a small range of potential differences.

In Fig. 2, we can easily see that, for $\mathcal{N} \gtrsim 9$ and $\gamma \lesssim 0.5$, the volt-ampere characteristic acquires the well-resolved shape of a ladder occupying the interval $0 < eV < 2$. The appearance of the first step in the current (or conductance) ladder of contacts with an

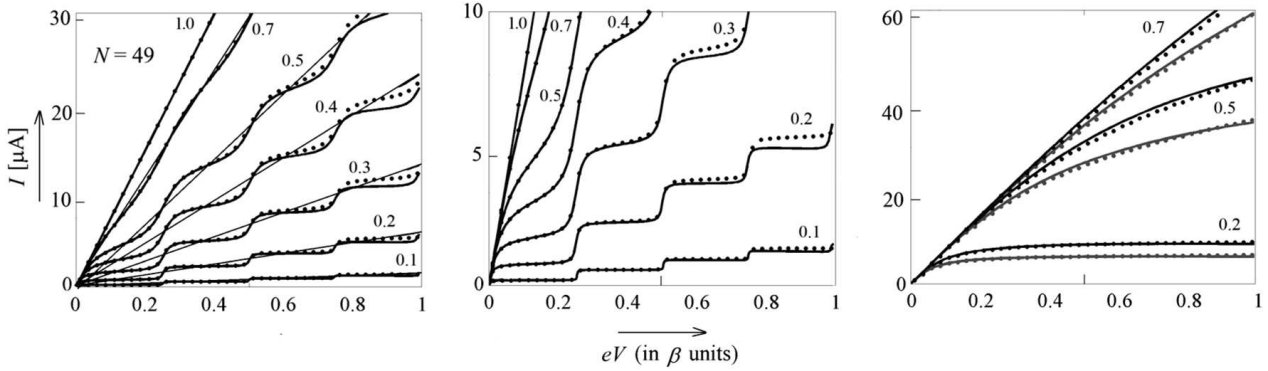


Fig. 4. Left panel: The exact dependence $I(eV)$ given by Eq. (21) is depicted by solid lines while its approximation (22) is displayed by dotted lines calculated for $\mathcal{N} = 49$, $\beta^{\text{cont}} = 1$ and $\gamma = 0.1, 0.2, 0.3, 0.4, 0.5, 0.7$, and 1.0 . Central panel: Enlarged dependences shown in the left panel. Right panel: The same dependences for $N = 3$ (black), $N = 5$ (red), and $\gamma = 0.2, 0.5$, and 0.7 .

odd number of atoms is associated with the state in the center of the contact spectrum $2 - eV/2$, i.e., with the central peak in the transmission spectrum and the only peak for which the transmission coefficient is equal to one for $E = 2 - eV/2$. The next steps in the ladder correspond to a pair of side resonances (i.e., two new states) appearing in the current window and, therefore, they are two times higher than the first step. In the transmission spectra of contacts with even numbers of atoms, the central peak is absent and, hence, all ladder steps have the same height. The presence-absence of the first and the lowest step in the conductance ladder serves as an indication of the odd-even effect on the conductance of weakly coupled contacts.

Similar features of the volt-ampere characteristics in the case $\beta^{\text{cont}} = \gamma$ can be observed in Fig. 3 (obviously, the curves for $\mathcal{N} = 1$ do not depend on β^{cont}). As can be seen by comparing the corresponding plots, the maximum values of currents are rather similar, i.e., they are mainly controlled by the values of the coupling parameter. The principal distinction between the cases $\beta^{\text{cont}} = 1$ and $\beta^{\text{cont}} = \gamma$ is the position of maxima, namely, for $\beta^{\text{cont}} = \gamma \lesssim 0.5$, the maxima are noticeably shifted toward lower values of eV .

4.3. Low potential difference

For the condition $eV \ll 1$, the obtained approximation of the transmission coefficient (20) admits the exact integration. Namely, we get an explicit expression for the current as a function of the potential dif-

ference, γ , and \mathcal{N} :

$$I(eV) = \frac{2e}{h} \frac{8\gamma^2}{(\mathcal{N} + 1)(1 + \gamma^4)} \times \arctan \left\{ \frac{1 + \gamma^4}{2\gamma^2} \tan \left[p + \frac{(\mathcal{N} + 1)eV}{4} \right] \right\}, \quad (22)$$

if $eV \lesssim 1$. As shown in Fig. 4, this approximation works reasonably well for $0 < eV \lesssim 1$. Thus, the simple analytic approximation (22) satisfactorily reproduces the current-voltage dependences for the molecular contact depicted in Fig. 1 as functions of the coupling parameter and contact length for the potential differences varying from zero to several electron-volts.

Note that, setting $\gamma = 1$ in the argument of arctan, we get a rough but reasonable approximation

$$I(eV) \approx \frac{2\gamma^2}{1 + \gamma^4} \frac{2e^2}{h} V, \quad eV \lesssim 1. \quad (23)$$

In particular, this gives the same result $I(eV) = \frac{2e^2}{h} V$ for $\gamma = 1$, which follows from Eq. (22). However, Eq. (23) does not reflect the ladder-type shape of I-V characteristics shown in Fig. 4, where the predictions of approximate equations are compared with the data of exact calculations.

The left and central panels in Fig. 4 accentuate the fact that the conductance ladder in long contacts can be observed if the contact region is weakly coupled with the emitter and collector. Two different current scales are used to demonstrate that the experimental observation of the conductance quantization requires to have the adequate sensitivity of current measurements. We also note that, for the potential difference

of interest (0.1–10 eV), the temperature effects are negligible up to the room temperature.

Unlike the contacts with large number of atoms, the I–V characteristics of short contacts shown in the right panel, have a structureless form. Two of these represent contacts $\mathcal{N} = 3, 5$, $\gamma = 0.2$, and exhibit a pronounced trend to saturation following the initial current growth. However, in the larger interval of potential difference, the I–V characteristics of the same contact pair $\mathcal{N} = 3-5$, in the bottom-mid panel in Fig. 2, exhibit noticeably different behavior. These and other examples discussed above demonstrate that even the simplest contact designs on the atomic level suggest a great variety of the electronic characteristics of nanosize devices.

5. Conclusions

In conclusion, we note that the exact and approximate expressions for the transmission coefficient and the current-voltage relations are found for the Wannier–Stark ladder of interacting levels. The analytic expressions for the transmission coefficient are obtained for the zero-temperature current through atomic wires. The constructed I–V characteristics are exact and accompanied by sufficiently accurate explicit approximate expressions.

Since atomic wires of different lengths are now real objects [27, 28], the reported properties of the I–V behavior are supposed to be observed in the course of experimental investigations of molecular contacts of the “metal-molecular chain-metal” type.

The author is grateful to the referee whose valuable suggestions helped to significantly improve the original version of the paper.

1. V. Mujica, M. Kemp, M. A. Ratner. Electron conduction in molecular wires. I. A scattering formalism. *J. Chem. Phys.* **101**, 6849 (1994).
2. S. Datta. *Electronic Transport In Mesoscopic Systems* (Cambridge University Press, 1995) [ISBN: 0521599431].
3. A. Onipko, Yu. Klymenko, L. Malysheva. Conductance of molecular wires: Analytical modeling of connection to leads. *Phys. Rev. B* **62**, 10480 (2000).
4. A. Nitzan. Electron transmission through molecules and molecular interfaces. *Annu. Rev. Phys. Chem.* **52**, 681 (2001).
5. V. Mujica, A. Nitzan, S. Datta, M.A. Ratner, C.P. Ku-biak. Molecular wire junctions: Tuning the conductance. *J. Phys. Chem. B* **107**, 91 (2003).
6. S. Datta. *Quantum Transport: Atom to Transistor* (Cambridge University Press, 2005) [ISBN: 0511643748].
7. A. Onipko, L. Malysheva. Coherent electron transport in molecular contacts: A case of tractable modeling. In: *Handbook on Nano- and Molecular Electronics*, Chapter 23 (CRC Press, 2007) [ISBN: 978-0-8493-8528-5].
8. A. Landau, L. Kronik, A. Nitzan. Cooperative effects in molecular conduction. *J. Comp. Theor. Nanoscience* **5**, 535 (2008).
9. E.G. Petrov. Modified superexchange model for electron tunneling across the terminated molecular wire. *Phys. Status Solidi B* **256**, 1900092 (2019).
10. E.G. Petrov, Ye.V. Shevchenko, V. Snitsarev, V.V. Gorbach, A.V. Ragulya, S. Lyubchik. Features of superexchange nonresonant tunneling conductance in anchored molecular wires. *AIP Advances* **9**, 115120 (2019).
11. G.H. Wannier. *Elements of Solid State Theory* (The University Press, 1960).
12. G.H. Wannier. Wave functions and effective Hamiltonian for Bloch electrons in an electric field. *Phys. Rev.* **117**, 432 (1960).
13. G.C. Stey, G. Gusman. Wannier-Stark ladders and the energy spectrum of an electron in a finite one dimensional crystal. *J. Phys. C: Solid State Phys.* **6**, 650 (1973).
14. H. Fukuyama, R.A. Bari, H.C. Fogedby. Tightly bound electrons in a uniform electric field. *Phys. Rev. B* **8**, 5579 (1973).
15. V.M. Yakovenko, H.-S. Goan. Edge and bulk electron states in a quasi-one-dimensional metal in a magnetic field: The semi-infinite Wannier-Stark ladder. *Phys. Rev. B* **58**, 8002 (1998).
16. Yu.B. Gaididei, A.A. Vakhnenko. Nonequilibrium kinetics of exciton wave packets in crystals. *Phys. Status Solidi B* **121**, 239 (1984).
17. S.G. Davison, R.A. English, A.L. Mišković, F.O. Goodman, A.T. Amos, B.L. Burrows. Recursive Green-function study of Wannier–Stark effect in tight-binding systems. *J. Phys.: Condens. Matter.* **9**, 6371 (1997).
18. A. Onipko, L. Malysheva. Triple-, double-, and fractionally-spaced Wannier-Stark ladders. *Solid State Commun.* **118**, 63 (2001).
19. A. Onipko, L. Malysheva. Noncanonical Wannier-Stark ladders and surface state quantization in finite crystals subjected to a homogeneous electric field. *Phys. Rev. B* **63**, 235410 (2001).
20. A. Onipko, L. Malysheva. Signatures of Wannier-Stark and surface states in electron tunneling and related phenomena: Electron transmission through a tilted band. *Phys. Rev. B* **64**, 195131 (2001).
21. A. Onipko, L. Malysheva. Analytic theory of Wannier-Stark quantization in arbitrary-size atomic square lattices. *Phys. Status Solidi B* 1700558 (2018).
22. L.I. Malysheva. Green function for a chain of interacting levels in the uniformly varying field. *Ukr. Fiz. Zh.* **45**, 1475 (2000).

23. R. Landauer. Spatial variation of currents and fields due to localized scatterers in metallic conduction. *IBM J. Res. Dev.* **1**, 223 (1957).
24. M. Büttiker, Y. Imry, R. Landauer, S. Pinhas. Generalized many-channel conductance formula with application to small rings. *Phys. Rev. B* **31**, 6207 (1985).
25. Y. Imry. *Introduction to Mesoscopic Physics* (Oxford University Press, 2002) [ISBN: 0-19-8507380].
26. C. Caroli, R. Combescot, P. Nozières, D. Saint-James. Direct calculation of the tunneling current. *J. Phys. C* **4**, 916 (1971).
27. S. Fölsh, P. Hyldgaard, R. Koch, K.H. Ploog. Quantum confinement in monatomic Cu chains on Cu(111). *Phys. Rev. Lett.* **92**, 056803 (2004).
28. J.N. Crain, D.T. Pierce. End states in one-dimensional atom chains. *Science* **307**, 703 (2005). Received 28.03.24

Л.І. Маллишева

ПРО ЕЛЕКТРИЧНИЙ СТРУМ
ПРИ НУЛЬОВІЙ ТЕМПЕРАТУРІ ЧЕРЕЗ АТОМНИЙ
ЛАНЦЮЖОК ПІД ДІЄЮ ПОЛЯ, ЩО ЗМІНЮЄТЬСЯ
РІВНОМІРНО: ФОРМАЛІЗМ ФУНКЦІЙ ГРІНА

На основі формалізму теорії сильного зв'язку та техніки функцій Гріна одержано усі матричні елементи функцій Гріна для ланцюжка під дією поля, що змінюється рівномірно. Проаналізовано їх залежність від параметрів системи у контексті електронного транспорту через молекулярні системи.

Ключові слова: електронний транспорт, функції Гріна, коефіцієнт пропускання.